

Apactin is involved in remodeling of the actin cytoskeleton during regulated exocytosis

Chanderdeep Tandon², Robert C. De Lisle¹

Department of Anatomy and Cell Biology, University of Kansas School of Medicine, Kansas City, KS 66160, USA

Received December 17, 2003

Received in revised version January 30, 2004

Accepted January 30, 2004

Acinar cell; Pancreas; Muclin; Zymogen granule; Apical plasma membrane

Apactin is an 80-kDa type I membrane glycoprotein derived from pro-Muclin, a precursor that also gives rise to the zymogen granule protein Muclin. Previous work showed that apactin is efficiently removed from the regulated secretory pathway and targeted to the actin-rich apical plasma membrane of the pancreatic acinar cell. The cytosolic tail (C-Tail) of apactin consists of 16 amino acids, has Thr casein kinase II and Ser protein kinase C phosphorylation sites, and a C-terminal PDZ-binding domain. Secretory stimulation of acinar cells causes a decrease in Thr phosphorylation and an increase in Ser phosphorylation of apactin. Fusion peptides of the C-Tail domain pulldown actin, ezrin, and EBP50/NHERF in a phosphorylation-dependent manner. HIV TAT-C-Tail fusion peptides were used as dominant negative constructs on living pancreatic cells to study effects on the actin cytoskeleton. During secretory stimulation, TAT-C-Tail-Thr/Asp phosphomimetic peptide caused an increase in actin-coated zymogen granules at the apical surface, while TAT-C-Tail-S/D phosphomimetic peptide caused a broadening of the actin cytoskeleton. These data indicate that stimulation-mediated Thr dephosphorylation allows decreased association of apactin with EBP50/NHERF and fosters actin remodeling to coat zymogen granules. Stimulation-mediated Ser phosphorylation increases apactin association with the actin cytoskeleton, maintaining tight bundling of actin microfilaments at the apical surface. Thus, apactin is involved in remodeling the apical cytoskeleton during regulated exocytosis in a manner controlled by phosphorylation of the apactin C-Tail.

Introduction

The actin cytoskeleton is well developed at the apical plasma membrane of the pancreatic acinar cell and has important roles in various cellular processes, especially membrane traffic in the exocytic and endocytic pathways (Muallem et al., 1995; Valentijn et al., 1999a). During regulated secretion the actin cytoskeleton undergoes remodeling (Valentijn et al., 1999a) but what controls these events is largely unknown. One aspect of remodeling in acinar cells is that actin is reorganized to enclose zymogen granules near the plasma membrane during exocytosis (Segawa and Yamashima, 1989; Valentijn et al., 2000). Exocytosis is followed by contraction of actin and myosin that helps maintain the apical plasma membrane and provides the force to expel exocytosed proteins into the ductal lumen (Segawa and Yamashima, 1989; Torgerson and McNiven, 2000; Valentijn et al., 1999b).

This report focuses on apactin (pronounced ap-actin) which was formerly referred to as p80 and is now renamed to indicate it is an apical actin cytoskeleton-associated protein. Apactin is generated in parallel with Muclin from a common precursor, pro-Muclin. pro-Muclin is a high-molecular-weight O-glycosylated, sulfated membrane glycoprotein that traffics through the secretory pathway and is proposed to have a role in aggregation/sorting of regulated secretory proteins at the trans Golgi network of the acinar cell (De Lisle and Ziemer, 2000; De Lisle, 2002). pro-Muclin is cleaved after leaving the Golgi, presumably in the immature secretory granule, liberating apactin, which consists of a 16-amino-acid cytosolic domain, a membrane-spanning domain, and a glycosylated luminal domain with a peptide core of about 65 kDa (De Lisle and Ziemer, 2000). Muclin remains in the mature zymogen granule associated with the protein content of the granule while apactin is efficiently removed to the apical plasma membrane.

The carboxy-terminal amino acids of apactin (-STKL-COOH) are predicted to form a type I PDZ (Postsynaptic density protein 95/*Drosophila* Disks large/Zonula occludens 1)-binding domain (Sheng and Sala, 2001), similar to that of CFTR (the cystic fibrosis conductance transmembrane regulator protein) (-DTRL-COOH). The C-terminus of CFTR

¹ **Corresponding author:** Dr. Robert C. De Lisle, Anatomy and Cell Biology, University of Kansas School of Medicine, 3901 Rainbow Blvd., Kansas City, KS 66160, USA, e-mail: rdelisle@kumc.edu, Fax: ++913 588 2710.

² Present address: Jaypee University of Information Technology, Waknaghat, Solan (H.P.), India.

interacts with a PDZ domain in EBP50/NHERF [ERM (Ezrin, Radixin, Moesin)-binding phosphoprotein 50/sodium-hydrogen exchange regulatory factor] (Milewski et al., 2001). This association has been reported to be necessary for apical localization of CFTR (Moyer et al., 2000), but other studies indicate that the association of the CFTR cytosolic tail with EBP50/NHERF stabilizes CFTR by increasing recycling to the plasma membrane after endocytosis (Swiatecka-Urban et al., 2002). In general, PDZ proteins function as organizers of protein complexes at the plasma membrane (Fanning and Anderson, 1999). The apectin C-Tail also has two predicted phosphorylation sites which potentially provide a means for sophisticated control of protein-protein interactions between the C-Tail and structural or regulatory elements in the cell. Therefore, in this work we explored mechanisms for targeting of apectin, focusing on its potential to associate with EBP50/NHERF and the well-developed actin cytoskeleton at the apical pole of the acinar cell. Also investigated was whether phosphorylation of apectin affects such interactions. The results show that the apectin C-Tail interacts with the actin cytoskeleton and has a phosphorylation-dependent role in remodeling of the actin cytoskeleton during regulated exocytosis in the acinar cell.

Materials and methods

Generation of GST and HIV-TAT constructs and purification of fusion proteins

Fusion proteins containing the wild-type apectin C-Tail and phosphomimetic mutants were generated by using overlapping oligonucleotides coding for the C-Tail peptides with overhangs complementary to restriction sites in the multiple cloning sites of the plasmids. For GST fusion proteins, the pGEX-4T plasmid was used, and for the HIV-TAT containing fusion proteins, the pTAT-HA bacterial expression vector was used (Vocero-Akbani et al., 2001). All constructs were verified by DNA sequencing. Both plasmids have the lac repressor, and fusion protein expression was induced in *E. coli* with IPTG. GST fusion proteins were solubilized from cell pellets of 10-ml cultures by sonication at 4°C in 1 ml PBS. Supernatants (14,000g × 10 min) were applied to glutathione agarose (Sigma; St. Louis, MO, USA) and the bound fusion proteins were used in pulldown experiments (see below). HIV-TAT fusion proteins were solubilized from cell pellets of 500-ml cultures by sonication at 4°C in 160 ml of 20 mM Na₂HPO₄, pH 7.4, 0.5 M NaCl, 10 mM imidazole, 0.1% SDS. Supernatants (14,000g × 10 min) of solubilized cells containing the His₆ tag fusion proteins were applied to Ni-Chelating Sepharose Fast Flow (Amersham; Piscataway, NJ, USA), incubated for 30 min, followed by washing with 100 mM imidazole, and elution with 100 mM acetic acid (pH 2.0). The eluted material was neutralized with 100 mM ammonium acetate (pH 9.0), lyophilized to dryness, and dissolved in distilled water. The fusion proteins were >90% pure as assessed by 15% acrylamide Tricine-SDS-PAGE and subsequent Coomassie blue staining of the gels (not shown).

In vitro phosphorylation of TAT-C-Tail fusion proteins

Purified TAT-C-Tail fusion proteins were used to confirm the predicted phosphorylation sites using [γ -³²P]ATP and purified casein kinase II (CKII) and protein kinase C (PKC) (Sigma, St. Louis, MO). Purified recombinant proteins were incubated with [γ -³²P]ATP and CKII according to (Woodgett, 1991) or PKC according to (Ogita et al., 1991). The labeled fusion proteins were then separated on 15% acrylamide Tricine gels, fixed, dried, and phosphorimaged (Cyclone; Packard Instruments, Meriden, CT, USA).

Preparation of pancreatic acini: in vivo ³²P-phosphorylation and [³⁵S]met/cys pulse-chase analysis

Pancreata from mice (ND4, Swiss Webster strain, Harlan, Indianapolis, IN) were digested with purified collagenase and then dissociated into acini as described previously (De Lisle and Bansal, 1996). To follow phosphorylation of the C-Tail of apectin in vivo, isolated acini (1/3 of cells from one mouse pancreas) were suspended in 3 ml phosphate-free HEPES-buffered Ringer's, preincubated 30 min, then resuspended in fresh phosphate-free buffer supplemented with 5 mCi [³²P]phosphate. The cells were aliquotted at 0.25 ml per well into 24-well plates and incubated 60 min at 37°C to allow labeling of cellular ATP pools. A secretory stimulus (1 μ M carbachol plus 1 mM 8-Br-cAMP, final) was added and the incubation was continued. Cells were harvested at the indicated times and solubilized by sonication on ice in RIPA (25 mM Tris-HCl, pH 7.4, with 50 mM NaCl, 0.1% SDS, 1% Triton X-100 and 1% deoxycholate) plus 10 mM EDTA, 0.1 M NaF, 2 mM pyrophosphate, and 50 μ M phenylarsine oxide. The sonicates were immunoprecipitated using the anti-C-Tail antibody as described (De Lisle and Ziemer, 2000), run on 7.5% acrylamide gels, transferred to PVDF membranes, and phosphorimaged. The labeled apectin bands were excised from the membrane, hydrolyzed in 6 N HCl for 1 h at 110°C, and liberated amino acids were analyzed by two-dimensional thin layer electrophoresis to determine the relative amounts of ³²P-phosphorylated Thr and Ser according to (Duclos et al., 1991).

To follow processing of newly synthesized pro-Muclin and the effects of the TAT-C-Tail fusion proteins, pancreas was digested with collagenase in met/cys-free medium, and the isolated acini were pulse-labeled in the presence of 0.5 mCi/ml [³⁵S]met/cys (Trans³⁵S-Label, ICN, Costa Mesa, CA) for 30 min. The cells were washed, aliquotted, and chased for the indicated times in the presence of no peptide or 0.3 μ M of the indicated TAT-C-Tail peptides. Cells were stimulated to secrete for 30 min after the 4-h time point (1 μ M carbachol plus 1 mM 8-Br-cAMP, final). The cells were transferred to siliconized microfuge tubes (Sigma) pelleted, and the cell pellets and media were saved. Media were precipitated with 10% trichloroacetic acid, dissolved in SDS sample buffer, separated by 10% SDS-PAGE, Coomassie blue stained, dried and phosphorimaged to quantify secreted ³⁵S-labeled amylase. The cell pellets (10% of the total) were separated by 7.5% SDS-PAGE and phosphorimaged to quantify cellular ³⁵S-labeled pro-Muclin and Muclin. ³⁵S-labeled apectin was immunoprecipitated using the anti-C-Tail antibody, separated by 10% SDS-PAGE, and phosphorimaged. Total protein bands were quantified using Optiquant Software (Packard Instruments) on scanned images of Coomassie blue-stained gels (Hewlett Packard ScanJet IICx; Palo, Alto, CA).

In some experiments release of prestored amylase was measured as enzyme activity in the culture medium samples using the amylase substrate ethylidene 4-nitrophenylmaltoheptaoside (Raichem; Columbia, MD, USA).

Pulldown assays, F-actin binding, and Western blot analysis

Mouse pancreas was homogenized in 10 mM Tris-HCl, pH 7.4, with protease inhibitors (1 μ g/ml pepstatin A, 1 μ g/ml leupeptin, and 200 μ g/ml pefabloc) and ultracentrifuged at 172,000g × 1 h to prepare cytosol. GST-C-Tail fusion proteins were bound to glutathione-agarose, washed, and incubated at room temperature for 10 min with 0.6 mg pancreatic cytosol in PBS, 10 mM sodium pyrophosphate, 100 mM sodium fluoride, 2 mM EDTA. After washing the beads bound proteins were separated by SDS-PAGE, transferred to PVDF membranes (Millipore; Billerica, MA, USA) and probed with antibodies to cytoskeletal proteins. Primary antibodies were used at the following dilutions: rabbit anti-actin (Sigma), 1:1000; rabbit anti-EBP50 [kind gift of Anthony Bretscher (Bretscher et al., 2000) and from Affinity Bioreagents, Inc.; Golden, CO, USA], 1:5000; and mouse anti-ezrin (Sigma), 1:1000. The secondary antibody for anti-actin was a goat anti-rabbit alkaline phosphatase conjugate (Jackson ImmunoResearch; West Grove, PA, USA) used at 1:1000 dilution and color was developed with nitroblue tetrazolium and bromo-chloro-indolylphosphate (Roche; Indianapolis, IN, USA). For

anti-EBP50 and anti-ezrin, the secondary antibodies were donkey anti-rabbit and -mouse horseradish peroxidase conjugates diluted 1:5000 and 1:1000, respectively (Jackson ImmunoResearch). The blots were processed for chemiluminescence using ECL reagent (Amersham; Arlington Heights, IL, USA) and images were collected on a chemi-imager (Alpha Inotech; San Leandro, CA, USA).

To test for the ability of apectin to bind directly to actin, an F-actin binding assay was used (catalog BK013, www.cytoskeleton.com). Monomeric non-muscle β -actin is polymerized at room temperature in the presence of Mg-ATP in 50 mM KCl. Then, GST-C-Tail peptides are added followed by a subsequent 30-min incubation at room temperature. The final concentration of actin is 18 μ M and the test peptides were all at a final concentration of 6.2 μ M. F-actin filaments are then pelleted by centrifugation at 150,000g \times 1.5 h at room temperature. Equal portions of the supernatants and pellets are analyzed by 10% acrylamide SDS-PAGE and Coomassie blue staining. The presence of the test peptide in the pellets is used to indicate association with F-actin. As a positive control for F-actin binding, α -actinin was used.

FITC-phalloidin labeling of the actin cytoskeleton and ezrin immunofluorescence

Pancreatic acini were incubated with no peptide or in the continuous presence of 0.3 μ M TAT-C-Tail peptides as indicated for one hour (basal), for 1 h followed by 0.5 h in the presence of 1 μ M carbachol plus 1 mM 8-Br-cAMP (stimulated), or for 1 h followed by 0.5 h plus stimulus followed by washing two times and a final 0.5-h incubation in the presence of 0.1 mM atropine to stop secretion (recovered). The cells were fixed in suspension for 0.5 h with 2% paraformaldehyde in PBS containing 0.1% saponin to permeabilize cell membranes, and 1 mM MgCl₂ and 5 mM EGTA to stabilize F-actin. After rinsing twice in PBS, the cells were incubated with 0.6 μ M FITC-phalloidin (Sigma) to label F-actin. The labeled acini were mounted with SlowFade (Molecular Probes, Eugene, OR, USA) and imaged on a Zeiss LSM510 confocal microscope. Z-stack images were collected as 0.5- μ m optical sections and were assembled into projections.

FITC-phalloidin-labeled acini prepared as above were also labeled with the anti-ezrin antibody (1:100 dilution) and detected with donkey anti-mouse Texas Red secondary antibody (1:100, Jackson ImmunoResearch). The labeled acini were imaged on a Nikon Diaphot microscope equipped with a SPOT II camera (Diagnostic Instruments, Sterling Heights, MI, USA).

Results

The cytosolic tail of apectin can be phosphorylated in vitro and in vivo

The cytosolic tail (C-Tail) of apectin comprises 16 amino acids (-GRRTHIDRGQPPSTKL-COOH) and has consensus sites for Thr casein kinase II (THID) and Ser protein kinase C (STKL) phosphorylation. To determine whether these sites can serve as substrates for cellular kinases, His₆-tagged TAT-C-Tail fusion proteins were used for in vitro phosphorylation reactions with purified casein kinase II (CKII) and protein kinase C (PKC). As shown in Figure 1, the wild-type C-Tail peptide is ³²P-phosphorylated by purified CKII, and mutation of the predicted Thr phosphorylation site to Ala prevents phosphorylation by CKII. Similarly, the wild-type C-Tail peptide is ³²P-phosphorylated by purified PKC and mutation of the predicted Ser phosphorylation site to Ala prevents phosphorylation by PKC.

To demonstrate that the phosphorylation sites are used in vivo, acinar cells were incubated with sodium [³²P]phosphate to label cellular ATP pools followed by apectin immunoprecipitation. The apectin immunoprecipitate shows two labeled bands consistent with two phosphorylation sites (Fig. 2A). In

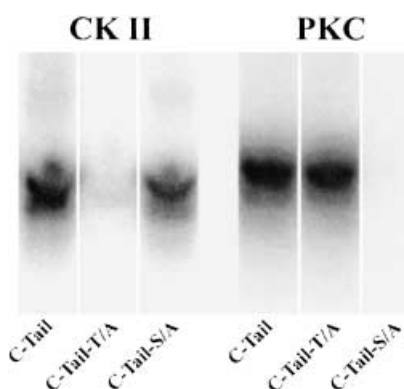


Fig. 1. In vitro phosphorylation of C-Tail fusion peptides. HIV-TAT fusion proteins containing the 16-amino-acid cytosolic tail of apectin were purified on Ni-chelating resin and incubated with [³²P]ATP plus purified casein kinase II (CKII) or protein kinase C (PKC). The samples were separated by SDS-PAGE followed by phosphorimaging. Mutation of the Thr and Ser to Ala in the kinase consensus sites prevented phosphorylation by CKII and PKC, respectively.

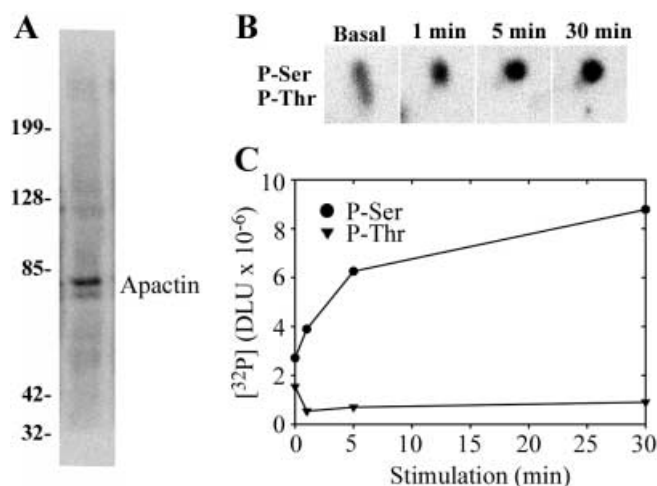


Fig. 2. The C-tail of apectin is phosphorylated in vivo. Isolated pancreatic acini were incubated with [³²P]phosphate to label cellular ATP pools. Apectin was immunoprecipitated from labeled cells, separated by SDS-PAGE, and phosphorimaged. (A) Two labeled bands are observed. (B) Two-dimensional thin layer electrophoresis analysis of phospho-amino acids from basal and stimulated acini. (C) Quantitation of ³²P-labeled Thr and Ser versus time of stimulation. Data are from a representative of two independent experiments. Data are presented as 'dynamic light units' (DLU) from the phosphorimager.

resting cells, by phosphoamino acid mapping (Fig. 2B), both sites are phosphorylated to different degrees, with almost twice as much label on the Ser PKC site as on the Thr CKII site (Fig. 2C). When the ³²P-labeled cells were stimulated to secrete there was a rapid decrease in ³²P-labeled Thr within 1 min of stimulation, and the level remained lowered as long as 30 min of stimulation (Fig. 2C). In contrast, there was an increase in ³²P-labeled Ser that was rapid for the first 5 min of stimulation and continued to increase at a slower rate as long as 30 min of stimulation (Fig. 2C). Immunoprecipitated pro-Muclin and mature Muclin from ³²P-labeled cells did not exhibit detectable phosphorylation (not shown).

The C-Tail of apactin binds to cytoskeletal proteins

Apactin is targeted to the apical plasma membrane in pancreatic acinar cells (De Lisle and Ziemer, 2000). To test whether apical localization of apactin might be through association of the C-Tail with cytoskeletal proteins, recombinant GST fusion proteins were prepared that represent the four possible phosphorylation states of the C-Tail: wild type (non-phosphorylated), T/D (single letter amino acid abbreviations) and S/D mono-phosphorylated phosphomimetics, and T&S/D dual-phosphorylated phosphomimetic. The fusion peptides were bound to glutathione agarose beads and used for pancreatic cytosol pulldown assays. Western blots were probed with antibodies for actin and the actin-associated proteins ezrin and EBP50/NHERF. The specificity of the antibodies and presence of these cytoskeletal proteins in the cytosolic preparation are shown in Figure 3A. In pulldown assays, actin was most strongly associated with the S/D phosphomimetic, less so by the T/D phosphomimetic, and much less by the wild type and T&S/D dual phosphomimetic proteins (Fig. 3B). Ezrin was weakly detected in the S/D pulldown and not in any of the others (Fig. 3B). All constructs pulled down EBP50/NHERF, with the wild type and T/D phosphomimetic constructs being the strongest (Fig. 3B).

To test whether apactin directly associates with actin, an F-actin binding assay was used with the GST-C-Tail fusion proteins (see Materials and methods). As shown in Figure 3C, none of the GST-C-Tail proteins were enriched in the F-actin pellets compared to a GST peptide alone. As a positive control, the known actin-binding protein α -actinin was used and all of this protein was in the F-actin pellet (Fig. 3C). Therefore, apactin is unlikely to directly bind actin although it does associate with the apical cytoskeleton.

Effects of TAT-C-Tail peptides on pro-Muclin processing to mature Muclin and apactin

Pro-Muclin traverses the regulated secretory pathway and undergoes proteolytic cleavage in a post-Golgi compartment to become mature Muclin and apactin (De Lisle and Ziemer, 2000). Pro-Muclin participates in zymogen granule formation, and the sulfated glycoprotein product Muclin, remains in the mature zymogen granules associated with the packaged digestive enzymes (De Lisle, 2002). To investigate whether the C-Tail of pro-Muclin/apactin is involved in TGN exit and vesicle trafficking steps, the protein transduction domain of the HIV-TAT protein (Vocero-Akbani et al., 2001) was used to prepare membrane-permeable C-Tail fusion peptides that were incubated with living pancreatic acini. These peptides are expected to act as dominant negative constructs and interfere with normal functioning of the C-Tail by competing for its binding partners. In preliminary experiments, a range of TAT-C-Tail peptide concentrations from 0.01 μ M to 20 μ M was tested (not shown). Lactate dehydrogenase (LDH) leakage was used to assess cytotoxicity of the TAT peptides. Cells incubated with 0–7 μ M of TAT peptide had about 3% of total LDH in the culture supernatant after 4 h incubation while those incubated with 20 μ M peptide had about 6% of total LDH in the culture supernatant after 4 h incubation (not shown). There were no differences in the effects of the TAT-C-Tail peptides at 0.3 μ M and 5 μ M for all the experiments described below. Therefore, the data presented here was obtained using 0.3 μ M, which is non-toxic to the cells.

To follow processing of pro-Muclin and production of mature Muclin and apactin in the presence of TAT-C-Tail peptides, isolated acini were pulse-labeled with [35 S]met/cys followed by chasing in the presence of the peptides. Pro-Muclin, mature Muclin, and apactin were visualized and quantified by phosphorimaging. The time course of disappearance of pro-Muclin (Fig. 4A, B) and appearance of mature Muclin (Fig. 4A, C) was not significantly affected by TAT peptide alone or TAT-C-Tail

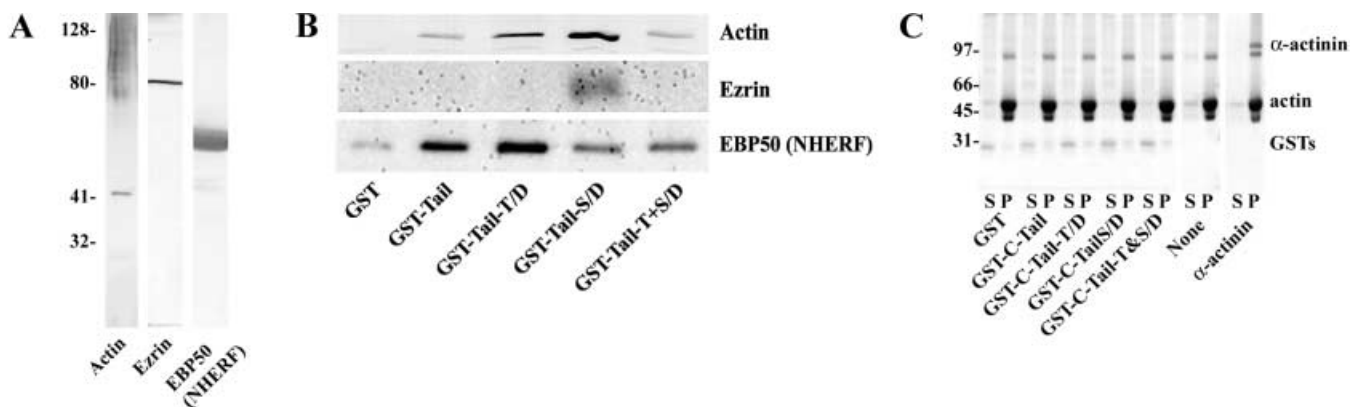


Fig. 3. The C-Tail of apactin associates with the cytoskeleton. (A) Specificity of the antibodies used. Pancreatic cytosol (50 μ g protein per lane) was separated by 10% SDS-PAGE, transferred to PVDF, and probed with the indicated antibodies. Actin, ezrin, and EBP50/NHERF are all present in the cytosol. (B) GST fusion protein pulldown assay. Equimolar amounts of the indicated GST-C-Tail fusion proteins bound to GSH-agarose were incubated with pancreatic homogenate. After washing the beads the proteins were separated by SDS-PAGE, transferred to PVDF, and probed with antibodies against actin, ezrin, and EBP50/NHERF. Actin and ezrin were pulled down most strongly by the C-Tail-S/D phosphomimetic peptide. EBP50/NHERF was

pulled down about equally by the wild-type C-Tail and the T/D phosphomimetic, with lesser amounts pulled down by the S/D phosphomimetic and the double phosphomimetic. Representative of 3–4 blots for each antibody. (C) The C-Tail of apactin does not directly bind actin. GST and GST-C-Tail fusion proteins were incubated with polymerized F-actin and pelleted. Equal portions of the supernatants (S) and pellets (P) were separated by SDS-PAGE and stained with Coomassie blue. Molecular weight markers are as indicated in kDa. None of the GST-C-Tail proteins are enriched in the F-actin pellets. The positive control, α -actinin, is highly enriched in the F-actin pellet. Representative of four repetitions.

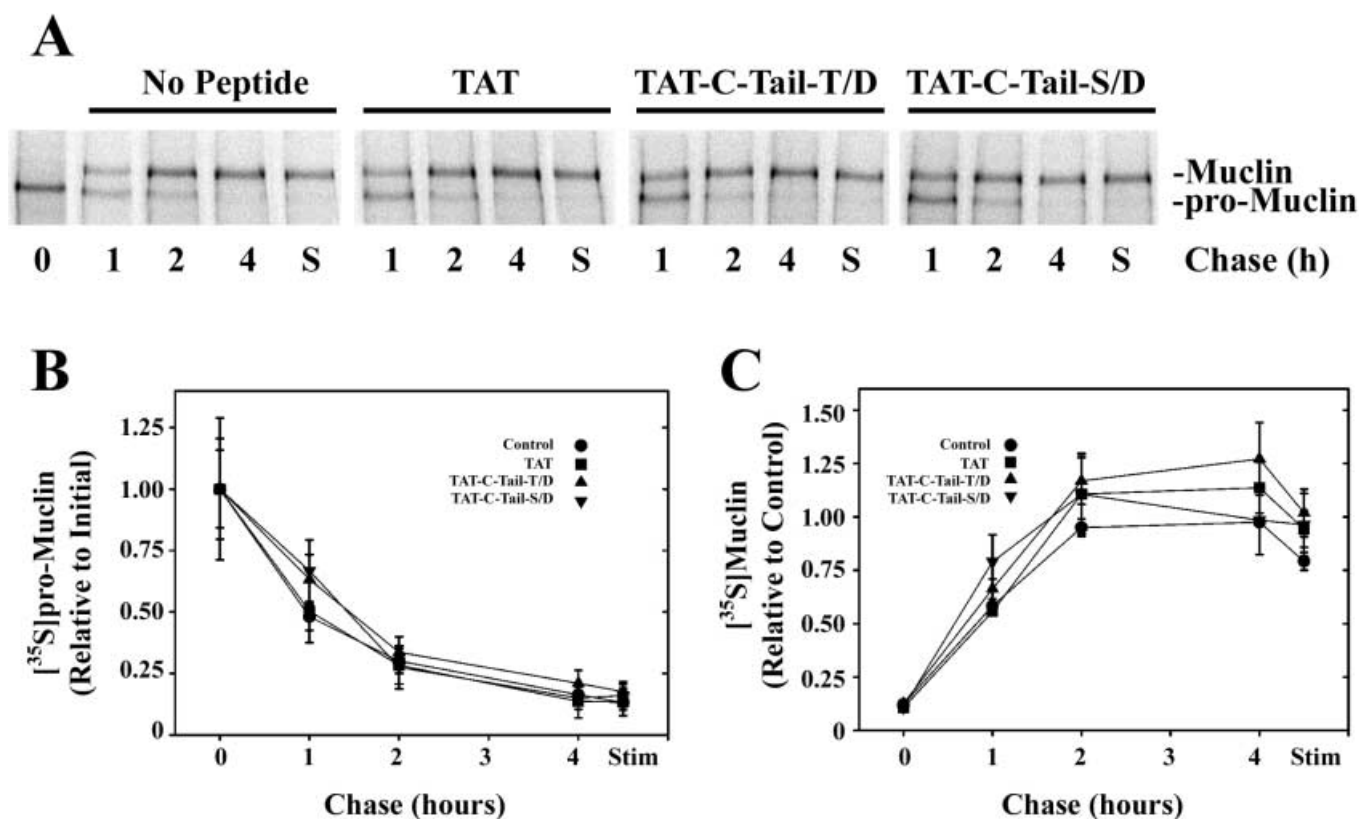


Fig. 4. Effect of TAT-C-Tail peptides on processing of pro-Muclin to mature Muclin. Pancreatic acini were pulse-labeled with [^{35}S]met/cys and chased in the presence of excess unlabeled amino acids and the indicated TAT-C-Tail peptides at 0.3 μM . (A) Radiolabeled pro-Muclin and mature Muclin were visualized by phosphorimaging of total cell protein samples separated by SDS-PAGE from representative experiments. The images show initial labeling of pro-Muclin (0) and decreasing levels during the chase (1–4). The final lanes are from

cells stimulated to secrete (S) for 0.5 h after a 4-h chase. Quantitation of radiolabeled pro-Muclin (B) and Muclin (C) as a function of chase time. None of the peptides had any significant effect on the kinetics of conversion of pro-Muclin to mature Muclin. Omitted for clarity, a TAT-wild type C-Tail peptide was also used and did not have any effect on processing of pro-Muclin to Muclin. The data are from five to eight independent experiments.

(not shown) nor by the phosphomimetics TAT-C-Tail-T/D and TAT-C-Tail-S/D. Since proteolytic cleavage occurs in a post-Golgi compartment (De Lisle, 2002), and the peptides did not interfere with the appearance of mature Muclin, it indicates that the C-Tail is not required for the exit of pro-Muclin from the TGN, or that a soluble C-Tail peptide does not fully compete with the membrane-bound native C-Tail.

In contrast to the lack of effect on pro-Muclin to Muclin maturation, these peptides affected levels of apactin. Untreated control cells accumulate ^{35}S -labeled apactin to a maximum level at 2 h of chase (Fig. 5), and exhibit a small decrease over the next 2 h of chase. When the cells are then stimulated to secrete there is little change in ^{35}S -labeled apactin levels during the 0.5-h period of stimulation. In contrast, in the presence of the wild-type TAT-C-Tail peptide there was a moderate increase in apactin accumulation at 4 h of chase and this increase persisted after the secretory stimulus (Fig. 5B). The TAT-C-Tail-T/D phosphomimetic had a larger effect on apactin accumulation which was increased to 150% and 172% of control levels at 2 and 4 h of chase, respectively (Fig. 5C). Remarkably, when stimulated the level of ^{35}S -labeled apactin in the presence of TAT-C-Tail-T/D returned to control levels (Fig. 5C). The TAT-C-Tail-S/D peptide was without a significant effect on apactin accumulation (Fig. 5D).

Effects of TAT-C-Tail peptides on basal and stimulated amylase release from acini

To investigate whether the TAT-C-Tail peptides affect stimulated release of zymogen granules, secretion of the abundant granule protein amylase was measured. Release of newly-synthesized protein that traversed the secretory pathway in the presence of the TAT peptides was measured using pulse-chase ^{35}S -labeled cells. These experiments used a long time course in the presence of the peptides to ensure that any effect of the peptides on trafficking of pulse-labeled protein would be observed. This requires that proteins traverse the secretory pathway through the Golgi complex and have time to be packaged into newly made mature zymogen granules. Maturation of pro-Muclin to mature Muclin and its incorporation into zymogen granules has a half-time of about 2 hours (De Lisle and Ziemer, 2000). As shown in Figure 6A, neither basal nor stimulated release of metabolically ^{35}S -labeled amylase was affected by TAT alone nor by TAT-C-Tail-T/D or -S/D peptides. The wild-type TAT-C-Tail was also used and was without effect on release of ^{35}S -labeled amylase (not shown).

To measure release of prestored amylase a shorter time course was used and enzyme activity in the media was determined. Similar to release of newly synthesized proteins, none of the peptides affected basal or stimulated release of pre-

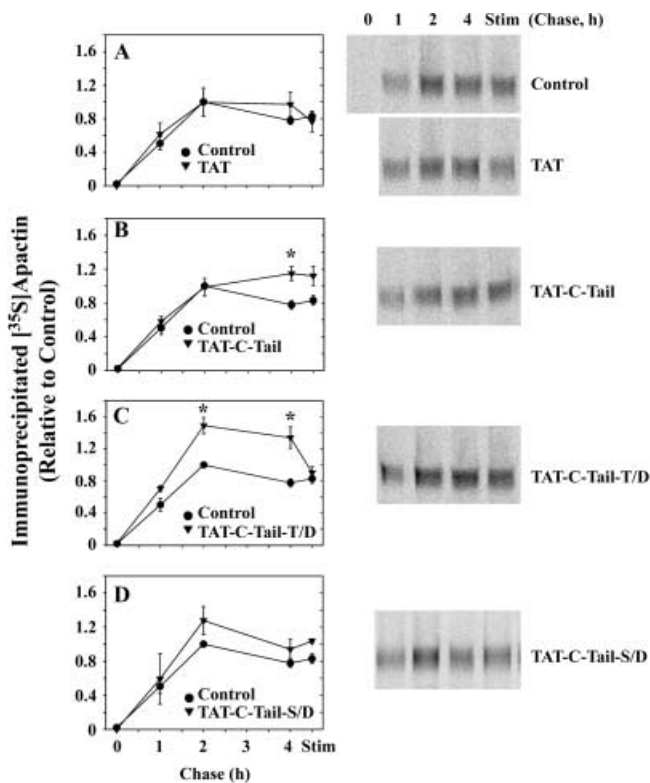


Fig. 5. Effect of TAT-C-Tail peptides on production of apactin from pro-Muclin. Apactin production and subsequent turnover were followed by C-Tail antibody immunoprecipitations, SDS-PAGE, and phosphorimage quantitation. At 4 h of chase the acini were stimulated to secrete protein. The data for Control are replicated in each panel to facilitate comparisons. (A) TAT peptide alone; (B) TAT-wild type C-Tail; (C) TAT-C-Tail-T/D mutation; (D) TAT-C-Tail-S/D mutation. Representative phosphorimages of immunoprecipitated ^{35}S -labeled apactin are shown on the right. The data were normalized to the control maximum signal, which occurred at the 2-h time point, to allow comparison of data from five to eight independent experiments. Asterisks indicate $P < 0.05$ vs. Control by ANOVA.

stored amylase, including the faster initial secretion (within 5 min) and the slower prolonged secretion (up to 60 min) (Fig. 6B). Thus, neither trafficking of secretory protein to the stimulatory pool, nor basal or stimulated release is affected by interfering with the C-Tail of apactin.

It is conceivable that the phosphomimetic peptides could exert an effect on amylase release after removal of the secretory stimulus or upon fresh stimulation. To test this, amylase release was measured during 30 min after the addition of atropine (100 μM) to stop carbachol-stimulated secretion. This treatment effectively reduced the amylase release rate to basal levels, but there was no difference in the presence of any of the TAT-C-Tail peptides (data not shown). When the cells were then further stimulated with 30 pM caerulein, amylase release resumed, but again was not affected by any of the TAT-C-Tail peptides (data not shown).

TAT-C-Tail-T/D and TAT-C-Tail-S/D phosphomimetics differentially affect the morphology of the actin cytoskeleton

The above experiments demonstrate that the C-Tail of apactin associates in an indirect manner with the actin cytoskeleton.

Therefore, we next examined whether interfering with the association of apactin with the actin cytoskeleton would alter the morphology of the actin cytoskeleton in isolated acini. Acini were incubated without or with 0.3 μM TAT-C-Tail peptides, and under basal, stimulated, and recovered conditions as described in Materials and methods, followed by F-actin labeling with FITC-phalloidin. The cells were then imaged as Z-series through the entire thickness of the acini on a confocal microscope and projection images were produced. Five separate experiments were performed with similar results.

When control acini were incubated under basal conditions and stained for F-actin, the majority of the signal was at the apical cell surface and the space between the cytoskeletons of neighboring cells across the shared lumen was fairly narrow (Fig. 7A). After stimulation of control acini the luminal space was broadened and there appeared occasional actin-decorated figures approximately 1 μm in size (arrow and inset in Fig. 7B). Segawa and Yamashina (1989) originally reported these structures in stimulated parotid acini, and Valentijn et al. (2000) showed in pancreatic acini that they are actin-coated zymogen granules that have not yet fused with the apical membrane. In stimulated control cells, about 30% had up to 10 actin-coated granules per acinus. After removal of the stimulus and allowing 0.5 h incubation for recovery, actin-coated zymogen granules were no longer observed, and the actin cytoskeleton surrounding the acinar lumen remained broadened (Fig. 7C) compared to unstimulated cells (Fig. 7A).

In the presence of TAT-C-Tail-T/D peptide under basal conditions the apical actin cytoskeleton had a similar morphology to controls (Fig. 7D). After secretory stimulation in the presence of this peptide there was an increase in the appearance of actin-coated zymogen granules (Fig. 7E). This effect was variable from acinus to acinus, which may be related to the fact that individual acini show differing degrees of activation when stimulated *in vitro* (Bosco et al., 1988; Valentijn et al., 2000). The example shown (Fig. 7E) is one of the more dramatic ones with virtually the entire lumen being lined with actin-coated granules. Overall, 75% of acini stimulated in the presence of TAT-C-Tail-T/D peptide had observable actin-coated zymogen granules. After recovery in the continued presence of the TAT-C-Tail-T/D peptide, actin-coated granules were not evident and the cytoskeleton remained broadened (Fig. 7F). In addition, there were F-actin-labeled dilations of about 5 μm diameter near the junctional complexes between lateral and apical membrane domains (arrowheads in Fig. 7F).

In the presence of TAT-C-Tail-S/D peptide under basal conditions there was a noticeable broadening of the actin cytoskeleton surrounding the acinar lumen (Fig. 7G). After secretory stimulation there was a further increase in the width of the cytoskeleton surrounding the lumen; the F-actin staining was quite diffuse and it appeared that the actin was less tightly bundled (Fig. 7H). Actin-coated zymogen granules were present but they were obscured by the broadened actin cytoskeleton. Overall, about 65% of acini stimulated in the presence of TAT-C-Tail-S/D peptide had a broadened actin cytoskeleton compared to about 13% in control acini. After recovery in the continued presence of the S/D peptide, the actin cytoskeleton remained broadened (Fig. 7I).

The effects of TAT-C-Tail peptides on EBP50/NHERF and ezrin were examined by immunofluorescence. Unfortunately, the anti-EBP50/NHERF did not work for immunofluorescence. For ezrin, the labeling pattern overlapped with F-actin, but the intensity of signal was weaker at the termini of the

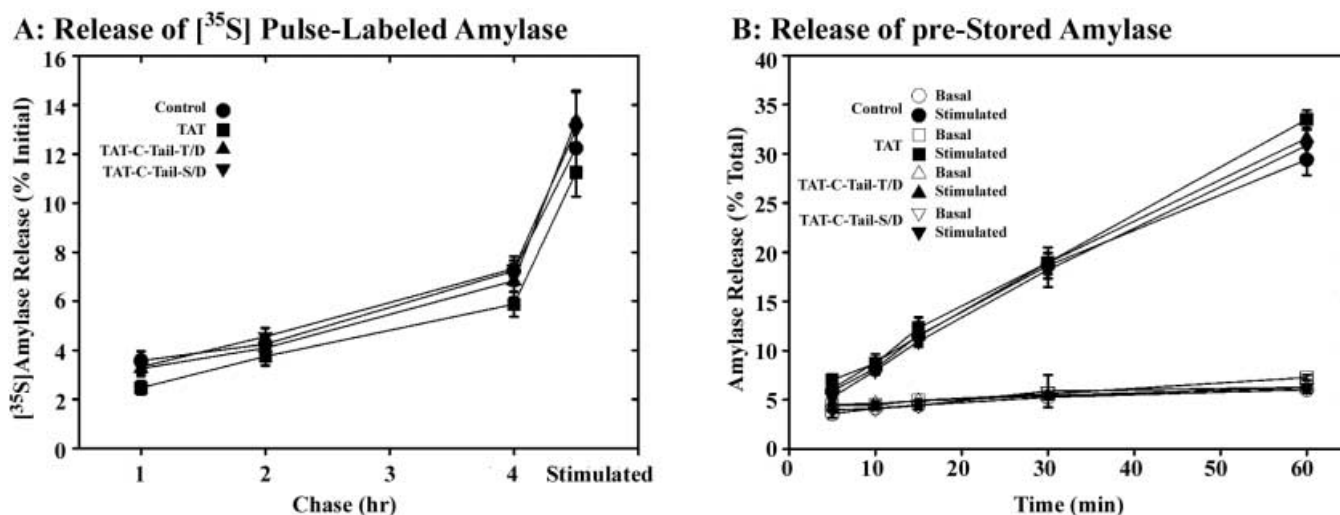


Fig. 6. Effect of TAT-C-Tail peptides on stimulated secretion of amylase. (A) Release of newly synthesized ³⁵S-labeled amylase. Acini were [³⁵S]met/cys pulse-labeled and chased in the presence of excess unlabeled amino acids and the indicated peptides (0.3 μM) for 4 h followed by an additional 0.5 h with a stimulus (Stimulated). The media were collected, separated by SDS-PAGE, and ³⁵S-labeled amylase was measured by phosphorimaging the gels. Values are shown for no peptide (Control), TAT peptide, TAT-C-Tail-T/D mutation, and TAT-C-Tail-S/D mutation. The TAT-wild type C-Tail peptide was also used and was without effect (omitted for clarity). Data are means ± SEM from 3–5 independent experiments per peptide. None of the peptides had any statistically significant effect on release of newly synthesized

amylase. (B) Release of pre-stored amylase. Acini were preincubated at 0.3 μM of the indicated peptides for 1 h. The cells were then incubated without (Basal) or with a stimulus (Stimulated) for another hour, with samples taken at the indicated times. Amylase enzyme activities in the media were determined and are expressed relative to the initial cell content. The data are means ± SD from quadruplicate samples of a representative experiment. Values are shown for TAT alone peptide, TAT-C-Tail-T/D mutation, and TAT-C-Tail-S/D mutation. The TAT-wild type C-Tail peptide was also used and was without effect (omitted for clarity). None of the peptides had any statistically significant effect on basal or stimulated release of pre-stored amylase.

apical surfaces compared to F-actin (Fig. 8A–C). Stimulation of the cells did not affect the ezrin labeling pattern in control cells (Fig. 8D–F). The TAT-C-Tail-T/D and -S/D peptides did not affect the ezrin labeling pattern under basal (Fig. 8G–I, M–O, respectively) or stimulated (Fig. 8J–L, P–R, respectively) conditions.

Discussion

The C-Tail of apactin is also present on pro-Muclin, the precursor to apactin and mature Muclin. Therefore, if the C-Tail has sorting or trafficking information it could operate in the secretory pathway before pro-Muclin is proteolytically cleaved as well as in post-Golgi compartments after liberation of apactin from pro-Muclin (De Lisle, 2002). We postulated that the C-Tail could serve in the formation of immature secretory granules at the TGN in a similar fashion as the cytosolic domains of the p24 family of endoplasmic reticulum cargo receptors function in egress from the ER (Belden and Barlowe, 2001). Using cell-permeant TAT-C-Tail peptides we tested this idea and found that there was no perturbation of the regulated secretory pathway in acinar cells.

Our previous work indicated an important role for the C-Tail (De Lisle and Ziemer, 2000). We showed that transiently transfected pro-Muclin was localized to sub-plasma membrane vesicles in rat pancreatic AR42J cells which increased storage of amylase. A pro-Muclin with the C-Tail deleted failed to form these vesicles and instead had small vesicles scattered throughout the cytosol (De Lisle and Ziemer, 2000). The fact that the

TAT-C-Tail peptides did not affect protein delivery to the regulated secretory pathway makes the role of the C-Tail less clear. It could be that the peptides, which are not membrane-associated as the native protein is, fail to effectively interfere with some C-Tail functions. Resolution of the importance of the C-Tail in protein sorting and granule formation will require further investigation.

In contrast to the lack of effect on passage of protein through the regulated pathway, peptides with a Thr/Asp mutation to mimic phosphorylation of the CKII site increased the accumulation of newly synthesized apactin in acinar cells. Pulse-chase analysis in control cells shows that apactin accumulation peaks at 2 h of chase and declines to a steady state at 4 h of chase, and that at this time the protein is stable even when the cells are stimulated. This suggests that a portion of newly made apactin is sorted to the apical plasma membrane (De Lisle and Ziemer, 2000) where it is fairly stable. Interestingly, the ‘excess’ apactin that accumulates in the presence of the T/D peptide is quite labile and is rapidly decreased to control levels. Attempts to determine where in the cell apactin accumulates (e.g., Golgi or plasma membrane) were unsuccessful (data not shown). Thus, trafficking of apactin in resting cells is influenced by CKII phosphorylation of the C-Tail, but in stimulated cells appears to be independent of the phosphorylation state of the CKII site.

The other major role postulated for the C-Tail of apactin was targeting to and association with the apical cytoskeleton. Using fusion proteins, it was shown that the C-Tail associates with a protein complex containing actin, ezrin, and EBP50/NHERF, and that these associations are modulated by the phosphorylation state of the C-Tail. Mutation of the Ser to Asp to mimic

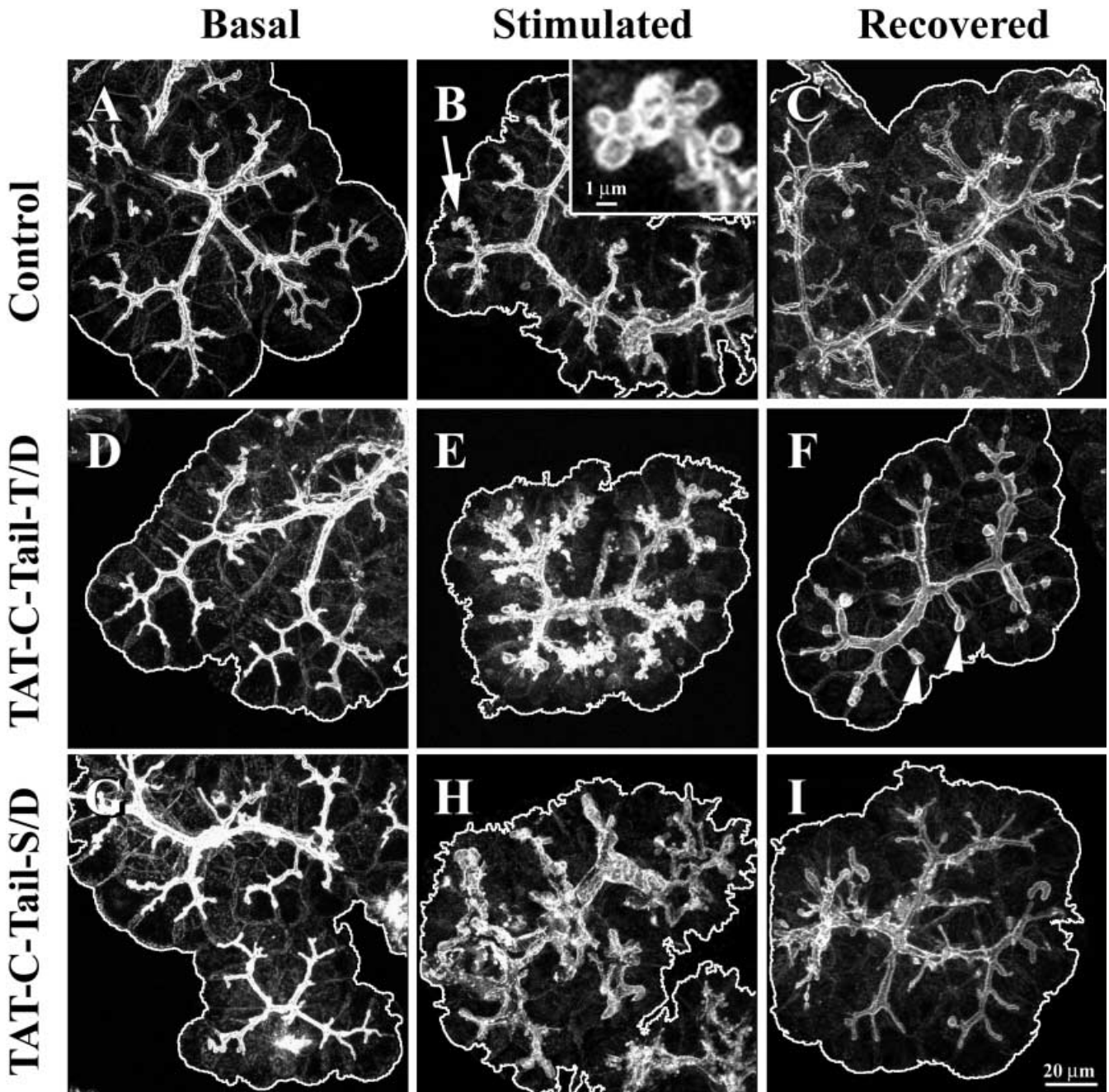


Fig. 7. Effects of TAT-C-Tail peptides on the F-actin cytoskeleton. Isolated acini were incubated at $0.3 \mu\text{M}$ of the indicated peptide for 60 min (Basal), followed by 30 min stimulation (Stimulated), and followed by washing and a further 30-min incubation step (Recovered). The cells were fixed, the actin cytoskeleton stained with FITC-phalloidin, and imaged on a confocal microscope. The images are projections of Z-series through the acini, and the peripheries of the acini are indicated by the white outlines. (A–C) No peptide control. (A) In the basal state the F-actin cytoskeleton surrounds the apical surface and is narrow. (B) In the stimulated state there appear small numbers of profiles of the size of zymogen granules (actin-coated zymogen granules) (arrow and inset). (C) After removal of the secretory stimulus the actin-coated zymogen granules disappear and the cytoskeleton largely returns to the basal appearance. (D–F) Acini

treated with $0.3 \mu\text{M}$ TAT-C-Tail-T/D phosphomimetic. (D) In the basal state the actin cytoskeleton is not noticeably different from the no-peptide control. (E) In the stimulated state there is a dramatic increase in the appearance of actin-coated zymogen granules. (F) After removal of the secretory stimulus, the actin cytoskeleton is dilated in appearance compared to control, and lateral actin-labeled figures of about $5 \mu\text{m}$ diameter are common (arrowheads). (G–I) Acini treated with $0.3 \mu\text{M}$ TAT-C-Tail-S/D phosphomimetic. (G) In the basal state the actin cytoskeleton is wider than the no-peptide control. (H) In the stimulated state there is a dramatic diffusion of the apical actin cytoskeleton. (I) After removal of the secretory stimulus the actin cytoskeleton returns to the basal state and remains widened compared to the no-peptide control.

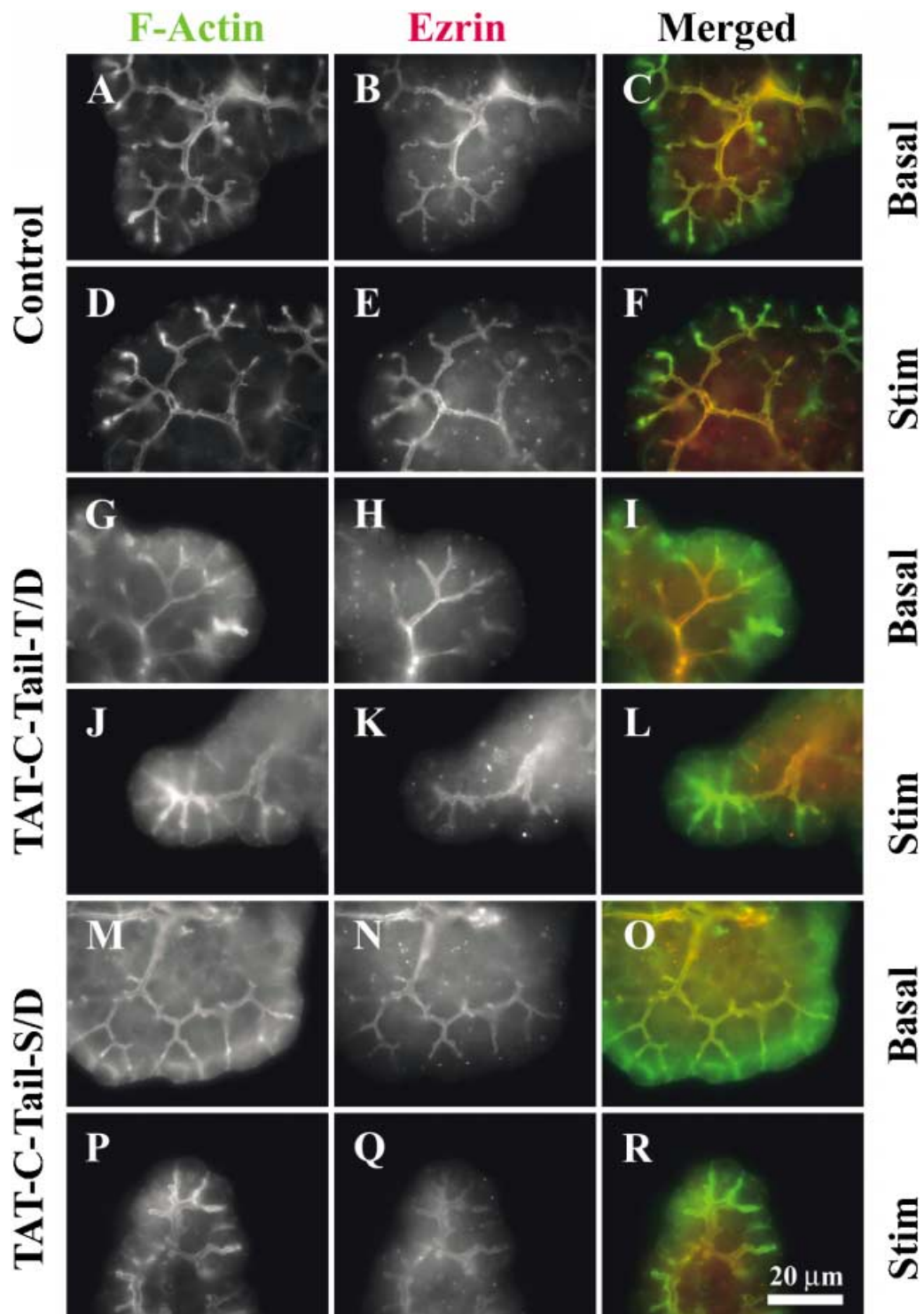


Fig. 8. Immunofluorescence staining for F-actin and ezrin. Isolated acini were prepared as in Figure 7 and dual stained for F-actin using FITC-phalloidin and ezrin using a monoclonal antibody with a donkey anti-mouse Texas Red secondary antibody. The labeled acini were imaged on a conventional fluorescence microscope. (A–C) Control, unstimulated (Basal). (D–F) Control, stimulated (Stim). (G–I) Acini treated with 0.3 μ M TAT-C-Tail-T/D phosphomimetic, unstimulated.

(J–L) Acini treated with 0.3 μ M TAT-C-Tail-T/D phosphomimetic, stimulated. (M–O) Acini treated with 0.3 μ M TAT-C-Tail-S/D phosphomimetic, unstimulated. (P–R) Acini treated with 0.3 μ M TAT-C-Tail-S/D phosphomimetic, stimulated. In all the acini, ezrin partially colocalizes with F-actin, except that ezrin staining is weaker at the termini of the apical surfaces. The ezrin staining pattern is not affected by secretory stimulation, nor by the TAT-C-Tail peptides.

PKC phosphorylation of the apactin C-Tail decreased EBP50/NHERF association compared to the wild-type C-terminus. This is consistent with previous work showing that phosphorylation of a Ser in this position of other PDZ-binding proteins decreases their binding affinity for PDZ domains [see (Sheng and Sala, 2001) for review]. On the other hand, mutation of the Thr to Asp to mimic CKII phosphorylation increased association of both actin and EBP50/NHERF compared to the wild-type C-terminus. Except for the PDZ protein EBP50/NHERF, direct binding partners for apactin have not been discovered yet. We tested whether the C-Tail of apactin could directly bind F-actin and found that it did not. Therefore, it remains to be determined how these differential associations with the apical cytoskeletal proteins are regulated.

To relate these data to what happens in the cell, phosphorylation of apactin *in vivo* was investigated. It was found that secretory stimulation changes the relative amounts of P-Thr and P-Ser: in the resting state the ratio of P-Thr to P-Ser was about 0.6 and when the cells were stimulated there was a rapid decrease in P-Thr and an increase in P-Ser. These data suggest that in stimulated cells apactin will have increased association with an actin-containing protein complex and decreased association with EBP50/NHERF.

The functional significance of the association of apactin with the actin cytoskeleton was investigated using TAT-C-Tail fusion peptides in live cells. These TAT-C-Tail peptides represent the cytosolic domain of apactin but lack the membrane and luminal domains. Therefore, they are expected to compete with the apactin C-Tail for association with other cell proteins, acting in a dominant negative fashion and revealing the roles of apactin in its different phosphorylated states. The TAT-T/D phosphomimetic, which competes with apactin for association with EBP50/NHERF, enhances actin-coating of zymogen granules in stimulated cells. Together, these data indicate that stimulation-dependent dephosphorylation of the apactin CKII site decreases its association with EBP50/NHERF, and in turn enhances remodeling of actin to coat zymogen granules near the apical plasma membrane.

The effects of the TAT-C-Tail-T/D peptide persisted after removal of the stimulus and there was an altered morphology of F-actin, with the appearance of 5- μm dilations near the junctional complex. It is expected that after removal of the stimulus apactin is rephosphorylated on the CKII site and reassociates with EBP50/NHERF. In the presence of the T/D peptide, this would be prevented by competition from the peptide and may interfere with reestablishment of the resting state of the actin cytoskeleton. The nature of these 5- μm structures is unclear but they may represent the actin-coats of several zymogen granules that become continuous after exocytosis of the granules in the presence of the peptide.

In contrast to the T/D peptide, the TAT-S/D peptide, which competes for the association of apactin with the actin cytoskeleton, results in broadening of the actin microfilaments, in resting cells and more dramatically during stimulation. Because stimulation increases phosphorylation of the apactin PKC Ser site and is expected to increase its association with actin, apactin will be more tightly associated with actin microfilaments keeping them close to the apical membrane during stimulated exocytosis. This might serve to keep the actin cytoskeleton cohesive at the apical plasma membrane while it is undergoing remodeling during stimulated exocytosis, and to help maintain the integrity of the luminal space as granule membrane is added to the plasma membrane.

The TAT-C-Tail peptides have a more pronounced effect on F-actin organization during secretory stimulation than in resting cells. This may be because the actin cytoskeleton is relatively static in the resting cell and that interactions with apactin only become apparent while it is undergoing remodeling during stimulation. The changes persisted to a degree after removal of the stimulus, suggesting that the peptides could continue to interfere with the association of native apactin with the cytoskeleton and to some extent prevent its remodeling back to the resting state.

Interestingly, the TAT-C-Tail peptides did not affect stimulated protein release from zymogen granules. The actin cytoskeleton is a barrier to secretory granule access to the plasma membrane as well as a necessary cell structure for regulated exocytosis [for review see (Burgoyne and Morgan, 2003)]. In the pancreatic acinar cell there are some conflicting data about whether agents that affect actin polymerization inhibit stimulated secretion. However, in toto, the data are convincing that zymogen granule exocytosis is actin cytoskeleton dependent [see (Torgerson and McNiven, 2000) for discussion of this issue]. For example, there is strong inhibition of release by the actin-depolymerizing cytochalasins (Burnham and Williams, 1982; John et al., 1983), by latrunculin A which inhibits actin polymerization (Torgerson and McNiven, 2000), and by the F-actin-stabilizing drug jasplakinolide (Valentijn et al., 2000). Furthermore, in streptolysin O-permeabilized acini, monomeric actin-binding proteins that lead to actin depolymerization stimulate secretion at basal $[\text{Ca}^{2+}]$ levels (Muallem et al., 1995).

During stimulation of acinar cells actin cytoskeleton remodeling results in coating of zymogen granules with filamentous actin before exocytosis (Valentijn et al., 2000). Valentijn et al. (2000) proposed that actin polymerization around zymogen granules is involved in the transport of granules through the apical actin cytoskeleton to the plasma membrane where exocytosis occurs. Segawa and Yamashina (1989) presented evidence that following granule-membrane fusion in salivary acinar cells, contraction of the actin surrounding granules provides the force to help expel the granule contents into the acinar lumen. This finding was more recently extended to pancreatic exocrine secretion by Valentijn et al. (2000). Further evidence for a mechanical role of actin-myosin contraction comes from a study where the myosin light chain kinase inhibitor ML-9 and the myosin II ATPase inhibitor butanedione monoxime were used and they were shown to inhibit F-actin remodeling as well as stimulated protein secretion (Torgerson and McNiven, 2000).

It might be predicted that enhancing the degree of actin-coated zymogen granules by the TAT-C-Tail-T/D peptide would increase amylase release. Since the T/D peptide did not affect amylase release, it indicates that this type of reorganization of the actin cytoskeleton is not a rate-limiting step in exocytosis in the acinar cell, nor does it interfere with exocytosis. Similarly, it might be predicted that disorganization of the actin cytoskeleton with the TAT-C-Tail-S/D would interfere with exocytosis. However, this peptide does not affect exocytosis, indicating that maintenance of the association of the luminal membrane via apactin and the actin cytoskeleton is not a requisite for exocytosis. An alternative function for apactin may be in compensatory endocytosis that follows exocytosis of zymogen granules (Valentijn et al., 1999a). This process is important for retrieving granule membranes and restoring the surface area of the apical plasma membrane after exocytosis.

This process is difficult to measure in pancreatic acini due to the geometry of acinar cell clusters and the limited accessibility of the apical membrane to probes (see Figs. 7, 8). Exploration of whether apactin has a role in compensatory endocytosis will require a more amenable model system than freshly isolated pancreatic acini.

In summary, we demonstrated that the membrane phospho-protein apactin is associated with the acinar cell apical actin cytoskeleton and that this association is modulated by changes in the phosphorylation state of the apactin cytosolic tail. When the interactions of apactin with the cytoskeleton are interfered with, there are complex changes in F-actin organization, especially during stimulated secretion. The phosphorylation states of the two sites in the cytosolic domain of apactin are differentially affected by stimulation, and these changes appear to have significant roles in remodeling of the actin cytoskeleton that accompanies regulated exocytosis and possibly compensatory endocytosis in the acinar cell.

Acknowledgements. This work was supported by National Institutes of Health grant DK 55998 to R. C. De Lisle. We thank Dr. Anthony Bretscher for his generous gift of the anti-EBP50 antiserum, and Dr. William H. Kinsey for performing the two dimensional phosphoamino acid analyses.

References

- Belden, W. J., Barlowe, C., 2001. Distinct roles for the cytoplasmic tail sequences of Emp24p and Erv25p in transport between the endoplasmic reticulum and Golgi complex. *J. Biol. Chem.* 276, 43040–43048.
- Bosco, D., Chanson, M., Bruzzone, R., Meda, P., 1988. Visualization of amylase secretion from individual pancreatic acini. *Am. J. Physiol.* 254, G664–G670.
- Bretscher, A., Chambers, D., Nguyen, R., Reczek, D., 2000. ERM-merlin and EBP50 protein families in plasma membrane organization and function. *Annu. Rev. Cell Dev. Biol.* 16, 113–143.
- Burgoyne, R. D., Morgan, A., 2003. Secretory granule exocytosis. *Physiol. Rev.* 83, 581–632.
- Burnham, D. B., Williams, J. A., 1982. Effects of high concentrations of secretagogues on the morphology and secretory activity of the pancreas: a role for microfilaments. *Cell Tissue Res.* 222, 201–212.
- De Lisle, R. C., 2002. Role of sulfated O-linked glycoproteins in zymogen granule formation. *J. Cell Sci.* 115, 2941–2952.
- De Lisle, R. C., Bansal, R., 1996. Brefeldin A inhibits the constitutive-like secretion of a sulfated protein in pancreatic acinar cells. *Eur. J. Cell Biol.* 71, 62–71.
- De Lisle, R. C., Ziemer, D., 2000. Processing of pro-Mucln and divergent trafficking of its products to zymogen granules and the apical plasma membrane of pancreatic acinar cells. *Eur. J. Cell Biol.* 79, 892–904.
- Duclos, B., Marcandier, S., Cozzone, A. J., 1991. Chemical properties and separation of phosphoamino acids by thin-layer chromatography and/or electrophoresis. *Methods Enzymol.* 201, 10–21.
- Fanning, A. S., Anderson, J. M., 1999. PDZ domains: fundamental building blocks in the organization of protein complexes at the plasma membrane. *J. Clin. Invest.* 103, 767–772.
- John, S. M., Rathke, P. C., Kern, H. F., 1983. Effect of cytochalasin D on secretion by rat pancreatic acini. *Cell Biol. Int. Rep.* 7, 603–610.
- Milewski, M. I., Mickle, J. E., Forrest, J. K., Stafford, D. M., Moyer, B. D., Cheng, J., Guggino, W. B., Stanton, B. A., Cutting, G. R., 2001. A PDZ-binding motif is essential but not sufficient to localize the C terminus of CFTR to the apical membrane. *J. Cell Sci.* 114, 719–726.
- Moyer, B. D., Duhaime, M., Shaw, C., Denton, J., Reynolds, D., Karlson, K. H., Pfeiffer, J., Wang, S. S., Mickle, J. E., Milewski, M., Cutting, G. R., Guggino, W. B., Li, M., Stanton, B. A., 2000. The PDZ-interacting domain of cystic fibrosis transmembrane conductance regulator is required for functional expression in the apical plasma membrane. *J. Biol. Chem.* 275, 27069–27074.
- Muallem, S., Kwiatkowska, K., Xu, X., Yin, H. L., 1995. Actin filament disassembly is a sufficient final trigger for exocytosis in nonexcitable cells. *J. Cell Biol.* 128, 589–598.
- Ogita, K., Yoshitaka, O., Kikkawa, U., Nishizuka, Y., 1991. Expression, separation, and assay of protein kinase C subspecies. *Methods Enzymol.* 200, 228–234.
- Segawa, A., Yamashina, S., 1989. Roles of microfilaments in exocytosis: a new hypothesis. *Cell Struct. Funct.* 14, 531–544.
- Sheng, M., Sala, C., 2001. PDZ domains and the organization of supramolecular complexes. *Annu. Rev. Neurosci.* 24, 1–29.
- Swiatecka-Urban, A., Duhaime, M., Coutermarsh, B., Karlson, K. H., Collawn, J., Milewski, M., Cutting, G. R., Guggino, W. B., Langford, G., Stanton, B. A., 2002. PDZ domain interaction controls the endocytic recycling of the cystic fibrosis transmembrane conductance regulator. *J. Biol. Chem.* 277, 40099–40105.
- Torgerson, R. R., McNiven, M. A., 2000. Agonist-induced changes in cell shape during regulated secretion in rat pancreatic acini. *J. Cell. Physiol.* 182, 438–447.
- Valentijn, J. A., Valentijn, K., Pastore, L. M., Jamieson, J. D., 2000. Actin coating of secretory granules during regulated exocytosis correlates with the release of rab3D. *Proc. Natl. Acad. Sci. USA* 97, 1091–1095.
- Valentijn, K., Valentijn, J. A., Jamieson, J. D., 1999a. Role of actin in regulated exocytosis and compensatory membrane retrieval: Insights from an old acquaintance. *Biochem. Biophys. Res. Commun.* 266, 652–661.
- Valentijn, K. M., Gumkowski, F. D., Jamieson, J. D., 1999b. The subapical actin cytoskeleton regulates secretion and membrane retrieval in pancreatic acinar cells. *J. Cell Sci.* 112, 81–96.
- Vocero-Akbani, A., Chellaiah, M. A., Hruska, K. A., Dowdy, S. F., 2001. Protein transduction: Delivery of Tat-GTPase fusion proteins into mammalian cells. *Methods Enzymol.* 332, 36–49.
- Woodgett, J. R., 1991. Use of synthetic peptides mimicking phosphorylation sites for affinity purification of protein-serine kinases. *Methods Enzymol.* 200, 169–178.